



Published in final edited form as:

*IEEE J Biomed Health Inform.* 2017 January ; 21(1): 201–210. doi:10.1109/JBHI.2015.2500191.

## Reconstruction-based Digital Dental Occlusion of the Partially Edentulous Dentition

**Jian Zhang,**

Department of Diagnostic Radiology, Wake Forest Medical School, Winston-Salem, NC 27103, USA

**James J. Xia,**

Department of Oral and Maxillo-facial Surgery, The Methodist Hospital, Houston, TX 77030, USA

**Jianfu Li,** and

Department of Oral and Maxillo-facial Surgery, The Methodist Hospital, Houston, TX 77030, USA

**Xiaobo Zhou**

Department of Diagnostic Radiology, Wake Forest Medical School, Winston-Salem, NC 27103, USA

### Abstract

Partially edentulous dentition presents a challenging problem for the surgical planning of digital dental occlusion in the field of craniomaxillofacial surgery because of the incorrect maxillomandibular distance caused by missing teeth. We propose an innovative approach called *Dental Reconstruction with Symmetrical Teeth* (DRST) to achieve accurate dental occlusion for the partially edentulous cases. In this DRST approach, the rigid transformation between two symmetrical teeth existing on the left and right dental model is estimated through probabilistic point registration by matching the two shapes. With the estimated transformation, the partially edentulous space can be virtually filled with the teeth in its symmetrical position. Dental alignment is performed by digital dental occlusion reestablishment algorithm with the reconstructed complete dental model. Satisfactory reconstruction and occlusion results are demonstrated with the synthetic and real partially edentulous models.

### Index Terms

Partially Edentulous; Dental Occlusion; Dental Alignment; Symmetrical Teeth; Missing Teeth; Point Registration

## I. Introduction

Craniomaxillofacial (CMF) surgery [1]–[3] corrects the congenital and acquired deformities of the skull and face. Throughout the world, many patients suffer from these deformities and require surgical correction [4]–[6]. CMF surgery includes many subfields, such as dentofacial deformities [7], combat injuries [8], posttraumatic defects [9], and deformities of the temporomandibular joint [10]. Most of them require the establishment of dental occlusion, i.e., maximum intercuspation (MI) position [7], [10], [11]. Thus, the establishment of dental occlusion is a central problem in the field of CMF.

Nowadays, with the wide application of all types of computer-aided surgical simulation systems [12]–[15], the success of dental occlusion highly depends on a precise surgical plan. With much effort [16]–[19], accurate surgery plan of the dental occlusion of the maxilla and mandibula with full dentition can be achieved in [19].

However, in real life, some patients miss one or several natural teeth, which is called partially edentulous dentition that is a major public health problem worldwide [20], [21]. It is usually treated by dental implants, bridges, or denture [22]. If a patient has a permanent dental prosthesis (e.g., dental implant or bridge), this will be a nonissue. If a patient has temporary dental prosthesis (e.g., denture), it must be removed at the time of the surgery. If a patient suffered from trauma and needs immediate surgical treatment, dental implant option will not be immediately available due to the lengthy treatment process. Most importantly, in CMF surgery, surgeons and orthodontists often extract a patients premolars intentionally to gain the spaces for the treatment. The spaces of these extracted teeth should not be closed and are usually not restored until the entire treatment is completed. Unfortunately, majority of previous studies [16]–[19] on digital dental alignment falls on the full dentition situation. To our knowledge, there is no effort that has been devoted to digitally establish the dental occlusion with partially edentulous models. Accurately predicting the partially edentulous cases with the alignment algorithms developed for the dental model through full dentition is difficult because the dental occlusion of full dentition is based on iterative surface-based minimum distance mapping with collision constraints [19]. The partially edentulous space created by the missing teeth significantly increases both the local and the global minima during computation and consequently leads to the unfavorable alignment result. Therefore, a digital dental occlusion algorithm should be developed for the partially edentulous dentition and our proposed approach was developed to address these real clinical problems.

In this paper, we propose to solve the digital dental occlusion problem of the partially edentulous dentition by reconstructing the complete dentition, which is realized by implanting virtual teeth into the partially edentulous space. A successful dental reconstruction depends on an accurate virtual implantation, which includes two aspects. First, the size and shape of the implanted virtual teeth should fit the existing individual anatomy of the patient. Second, the implantation pose should be correct. The previous algorithm of dental occlusion reestablishment for the full dentition can be employed to align the reconstructed maxillary and mandibular models.

Previously, some algorithms for reconstructing the missing teeth [23]–[25] have been proposed. These methods are developed for chewing purpose instead of occlusion purpose, as required in this project. Most of them [23], [24] are proposed for restoring the broken crown caused by cavity. A decayed tooth should have remaining parts for it to be reconstructed. A tooth cannot be reconstructed if it is completely missing. A recent approach [25] is capable of handling both the broken crown and the whole missing teeth. First, a statistical teeth model is built from a selection of tooth shapes. Several landmarks on each training tooth surface should be manually marked beforehand. Then, the obtained tooth model is fitted into the concerned dental model with respect to the remnant of the broken crown or the neighboring teeth. This approach needs to process a number of dental models and cannot be run full automatically. Time-consuming manual labor is required in the

landmark manually marking step. Furthermore, the uniform tooth model calculated from a limited number of tooth shapes based on the manually assigned landmarks is hard to be adjusted to each individual patient's anatomy.

To address this challenging problem, we have developed a novel approach called *Dental Reconstruction with Symmetrical Teeth* (DRST), which makes profit of the symmetrical property of the dentition. The most suitable entity for filling the partially edentulous space is the original missing teeth, which can perfectly meet the anatomical requirements of each individual patient. However, we do not have the original teeth. Nonetheless, given that the dental model is bilaterally symmetrical for most people [26]–[28], with proper processing, the symmetrical teeth of the missing teeth can be employed to provide a substitute with high similarity to the original teeth. Consequently, a customized dental reconstruction can be expected. Fig. 1 shows the flowchart of the approach. After segmenting each tooth and the partially edentulous position of the dental model (Section III), the transformation, which is a combination of the mirror transformation, the rotation, and the translation, is estimated with a pair of teeth on both the left and right sides (Section IV-B) so that the implantation location can be precisely decided; Subsequently, the partially edentulous space is virtually filled with its symmetrical counterpart, which provides a perfect filling entity (Section IV-C).

Accordingly, this paper is organized as follows. In Section II, we describe the acquisition of digital dental data. The segmentation method is presented in Section III. We explain the DRST method theoretically in Section IV-A and present the detailed process in Sections IV-B and IV-C. Finally, we demonstrate the reconstructed dental models and validate the digital dental occlusion results with synthetic and real data in Section V.

## II. Data Acquisition and Preprocessing

The digital dental model (Fig. 2(a)) was obtained by scanning the physical dental model by a three dimensional (3D) laser surface scanner with an accuracy of  $0.1\text{mm}$  by a commercially available service (GeoDigm Corporation, Chanhassen, MN). The result was saved in stereolithography (.STL) format, where the 3D surface of each dental model is expressed by a triangulated mesh surface (Fig. 2(c)) consisting of facets and vertices. Each facet has a known normal vector going outwardly. Each vertex is shared by its known neighbouring facets. The vertices form a point cloud on the surface (Fig. 2(d)). A tooth or any component of the dental model is a collection of the corresponding facets and points. The set of maxillary and mandibular models of one patient was at MI relationship to provide ground truth for validation. The MI relationship was obtained with the physical dental models [7], which were hand-articulated by experienced CMF surgeons. The partially missing tooth or teeth could be easily ignored. This is the traditional way to establish the occlusion in the real world.

As in many dental studies [19], [29], the occlusal plane ( $x$ - $O$ - $y$  plane) of a set of dental models is defined by the distobuccal cusps of the two first molars and the incisal edge of a central incisor of the mandibular model. The  $y$ -axis is along the sagittal direction. The  $z$ -direction is superoinferior. The origin  $O$  of the *Cartesian* coordinate system is the centroid of

the boundary box of the mandibular model in MI position. We are interested only in the teeth-related part instead of the whole dental model. Hence, the maxillary model is cut by a cutting plane  $H$ , which is  $5\text{mm}$  higher than the occlusal plane. The points that are lower than the plane  $H$  are selected. The facets on the surface of the maxillary model, whose all three vertices are lower than the plane  $H$ , are selected. The mandibular model is cut by another cutting plane  $L$ , which is  $5\text{mm}$  lower than the occlusal plane. The points that are higher than the plane  $L$  are selected. The facets on the surface of the mandibular model, whose all three vertices are higher than the plane  $L$ , are selected. In the following sections, the dental model refers to the selected part (Fig. 2(b)) of the full model unless otherwise specified. The set of the dental model refers to the maxillary and mandibular dental model of the same patient. In our project, it is not necessary to discard the braces and orthodontic wires if the patient is under orthodontic treatment.

### III. Dental Segmentation

In our project, we are going to reestablish the MI relationship between the maxillary model and the mandibular model, where one tooth or several teeth are missing. Before we apply the DRST method, each tooth and the partially edentulous position in the dental model have to be identified. In this paper, a dental segmentation approach is developed, which figures out a sequence of spokes that separate each tooth and the partially edentulous position. The steps are as follows.

First, we compute a sequence of raw spokes. As in Fig. 3(a), a range image [30] of the partially edentulous teeth model in Fig. 2(b), whose gray value of each pixel represents the height of a sample point on the teeth model from the reference surface, can be obtained. Then, the dental arch curve, which is the black curve in Fig. 3(b), can be fitted with a fourth-order polynomial. Along the dental arch curve, a sequence of candidate spokes was set up equally, which are line segments perpendicular to the dental arch. The intersection of each spoke with the dental arch is called its arch points. With the algorithm proposed in [29], we obtain a raw sequence of spokes (Fig. 3(b)). According to this raw sequence, each two adjacent teeth has been properly segmented by a spoke that is correctly located in the interstices with a right angle. However, as the algorithm is developed for a full teeth set, no spoke indicates the boundary of the partially edentulous space, and some spokes are provided in the partially edentulous position by mistake. We will discuss these problems in the following steps.

We then develop a method to detect the partially edentulous space. We extract the gray value of the points sampled along the dental arch. The gray values of the sample points that are located in the partially edentulous position are much lower than the others due to the absence of the teeth. Thus, we can detect the partially edentulous position easily. The first and last of the sample points in the partially edentulous space are called the start and end points, respectively. The partially edentulous position is identified by the two articulated spokes (Fig. 3(c)), which are the line segments perpendicular to the arch curve and pass by the start and end points. Obviously, one partially edentulous position can have several missing teeth as long as it is continuous.

Finally, we combine the raw sequence with the partially edentulous position information to obtain a polished spoke sequence. We first filter the spokes in the partially edentulous position, which are all fake ones. Therefore, we delete the spokes whose arch points are between the start and end points. Then, we add the two articulated spokes to the spoke sequence and sort the spokes by the arch points. The polished spoke sequence (Fig. 3(d)) is obtained, which segments each tooth and the partially edentulous position decently.

#### IV. Dental Reconstruction with Symmetrical Teeth

In this section, we will present the method of DRST in detail. The central thought of DRST is to fill the partially edentulous space by reconstructing the missing tooth with its symmetrical tooth on the other side of the face. As a complete dental model is rigid and generally symmetrical, half of the dental model can be transformed to match the other half part as a whole. All of the points on the transformed surface share the same transformation. Consequently, the transformation of one tooth can be estimated with another tooth on the same side. Based on this knowledge, the DRST method is proposed to reconstruct the partially edentulous dental model. Then, we can reestablish the dental occlusion between the complete maxillary and mandibular model.

##### A. The Proposed Method

Let us consider a dental model with full dentition. Let  $\{U_j\}_{1 \leq j \leq M_1}$  be the 3D coordinates of the set of vertices in the left or right half of the dental model and  $\{V_j\}_{1 \leq j \leq N_1}$  be the 3D coordinates of the set of vertices in the other half of the dental model. In the theoretical ideal setting of perfectly mirrored point sets, the point cloud  $\{U_j\}$  is symmetrical with  $\{V_j\}$ . With the following rigid transformation  $\mu: \mathbb{R}^3 \rightarrow \mathbb{R}^3$  performed on  $\{V_j\}$ , we can match the two shapes.

The first step of the rigid transformation consists of flipping  $\{V_j\}$  by a mirror transformation, denoted by  $\mu_1: \mathbb{R}^3 \rightarrow \mathbb{R}^3$ . The mirror transformation is parameterized by a  $3 \times 3$  mirror transformation matrix  $M$ . The 3D coordinates of the mirrored  $\{V_j\}$  are denoted by  $\{W_j\}_{1 \leq j \leq N_1}$ . We have

$$W_i = \mu_1(V_i; M); \quad (1)$$

$$\mu_1(V_i; M) = MV_i. \quad (2)$$

The second step consists of applying a rotation and translation transformation  $\mu_2: \mathbb{R}^3 \rightarrow \mathbb{R}^3$ .  $\{\hat{W}_j\}_{1 \leq j \leq N_1}$  denotes the transformed  $\{W_j\}$ .  $\mu_2$  is parameterized by  $\Theta$ , which is given by a  $3 \times 3$  rotation matrix  $R$  and a  $3 \times 1$  translation vector  $t$  as follows:

$$\hat{W}_i = \mu_2(W_i; \Theta); \quad (3)$$

$$\mu_2(W_i; \Theta) = RW_i + t, \Theta := \{R, t\}. \quad (4)$$

$\Theta$  denotes the registration parameters [31]. Given  $\Theta$ ,  $\{W_j\}$  can be transformed to match  $\{U_j\}$ .

By combining (1), (2), (3), and (4), we have

$$\hat{W}_i = \mu(V_i; M, R, t); \quad (5)$$

$$\mu(V_i; M, R, t) = RMV_i + t. \quad (6)$$

(5) and (6) indicate that half of the dental model  $\{V_j\}$  can be transformed to match another half of the dental model  $\{U_j\}$  with the rigid transformation  $\mu$  parameterized by  $\{M, R, t\}$ . This is true for their subsets as well.

Suppose  $\{U'_m\}_{1 \leq m \leq M_2}$  is one tooth in  $\{U_j\}$ ,  $\{V'_n\}_{1 \leq n \leq N_2}$  is in  $\{V_i\}$ , and  $\{V'_n\}$  is the symmetrical tooth of  $\{U'_m\}$ . We have

$$\begin{aligned} \{U'_m\} &\in \{U_j\}; \\ \{V'_n\} &\in \{V_i\}. \end{aligned}$$

With the same rigid transformation  $\mu$  parameterized by  $\{M, R, t\}$  illustrated in (5) and (6), we have:

$$\begin{aligned} \hat{W}'_n &= RMV'_n + t; \\ \{\hat{W}'_n\} &\in \{\hat{W}_i\}, \quad (7) \end{aligned}$$

where  $\{\hat{W}'_n\}_{1 \leq n \leq N_2}$  is the tooth  $\{V'_n\}$  after the transformation  $\mu$ . It is a tooth in  $\{\hat{W}_i\}$ . As  $\{\hat{W}_i\}$  matches  $\{U_j\}$ ,  $\{\hat{W}'_n\}$  matches  $\{U'_m\}$ .

It is the same with another tooth  $\{U''_l\}_{1 \leq l \leq M_3}$  in  $\{U_j\}$  and its symmetrical tooth  $\{V''_k\}_{1 \leq k \leq N_3}$  in  $\{V_j\}$ :

$$\begin{aligned}
\{U_l''\} &\in \{U_j\}; \\
\{V_k''\} &\in \{V_i\}; \\
\hat{W}_k'' &= RMV_k'' + t; \\
\{\hat{W}_k''\} &\in \{\hat{W}_i\}, \quad (8)
\end{aligned}$$

where  $\{\hat{W}_k''\}_{1 \leq k \leq N_3}$  is the tooth  $\{V_k''\}$  after the same transformation  $\mu$  parameterized by  $\{M, R, t\}$ .  $\{\hat{W}_k''\}$  matches  $\{U_l''\}$ .

According to (7) and (8), with the same transformation  $\mu$  defined by  $M, R, t$ ,  $\{V_n'\}$  can be transformed to match  $\{U_m'\}$ , and  $\{V_k''\}$  can be transformed to match  $\{U_l''\}$ . Therefore, if  $\{U_l''\}$  is missing and we would like to fill the partially edentulous space  $E$  with its symmetrical tooth  $\{V_k''\}$ , we can estimate the rigid transformation with another teeth pair  $\{U_m'\}$  and  $\{V_n'\}$ , as long as they exist. The parameters  $\{M, R, t\}$  can be estimated by transforming  $\{V_n'\}$  to  $\{U_m'\}$  and then applied to transform  $\{V_k''\}$  to  $E$ . In practice,  $\{U_m'\}$ ,  $\{V_n'\}$ ,  $\{U_l''\}$ , and  $\{V_k''\}$  can represent several teeth. We assume that the teeth of most patients are symmetric and can be treated with the proposed approach.

## B. Estimate the Transformation

In this step, we estimate the transformation with a pair of teeth, which are symmetrical with each other. Several partially edentulous positions can exist in one dental model, denoted by  $E_a$  ( $a = 1, \dots, K$ ). From the previous discussion, all of the partially edentulous positions on one side can be filled by their symmetrical counterparts under the same transformation. However, to make the process more accurate, we recommend to estimate the transformation for each partially edentulous position  $E_a$  with the teeth close to  $E_a$ . We continue employing the dental model shown in Fig. 2(b) to explain the estimation. In this example, there is only one partially edentulous position, which is denoted by  $E$  as no ambiguity.

First, we should decide the teeth pair  $\{U_m'\}$  and  $\{V_n'\}$  from the remaining teeth. A continuous entity  $\{U_m'\}$  on the same side of  $E$ , which has one tooth or several teeth, can be selected, as long as its symmetrical counterpart exists on the other side. It would be much ideal if  $\{U_m'\}$  is close to  $E$ . For simplicity, we select only one tooth, i.e., the right first premolar as  $\{U_m'\}$  in this example. Then, its symmetrical tooth, the left first premolar, is selected as  $\{V_n'\}$ .  $\{U_m'\}$  and  $\{V_n'\}$  are called the source tooth and the symmetrical tooth, respectively.

$\{U_m'\}$  and  $\{V_n'\}$  can be segmented from the whole dental model with their left and right spoke planes. A spoke plane is a plane passing by a spoke line and is parallel to the  $z$ -axis. The vertices between two spoke planes are bounded and thus can be segmented. The facets whose all three vertices are between the two planes are segmented. As a result, the

triangulated mesh that represents the selected object is obtained. For example, in Fig. 4(a), the right first premolar and the left first premolar are segmented from the dental model, serve as  $\{U'_m\}$  and  $\{V'_n\}$ , and are marked as red mesh and pink mesh, respectively.

Then, the symmetrical tooth  $\{V'_n\}$  can be flipped to the same side of  $\{U'_m\}$  by a mirror transformation  $\mu_1$ . The mirrored tooth  $\{W'_n\}$  can be computed as follows:

$$W'_n = MV'_n, \quad (9)$$

where

$$M = \begin{pmatrix} -1 & 0 & 0 \\ 0 & 1 & 0 \\ 0 & 0 & 1 \end{pmatrix} \quad (10)$$

because the mirror transformation is about the  $y$ - $O$ - $z$  plane under the coordinate system presented in Section II.

The mirrored tooth  $\{W'_n\}$  is marked as blue mesh, as shown in Fig. 4(b). However, it does not match the source tooth  $\{U'_m\}$ . We will perform a rigid transformation  $\mu_2$  on  $\{W'_n\}$  and match the two shapes. This problem becomes the point registration problem, which aims (i) to find point-to-point correspondence between two sets of points and (ii) to estimate the transformation that allows the alignment of the two sets. Numerous algorithms [32]–[35] have been proposed to address this issue. In our project, we adopt the *Expectation Conditional Maximization for point registration* (ECMPR) algorithm [31] to match the two rigid shapes and to estimate the transformation  $\mu_2$  performed on  $\{W'_n\}$ , which is defined by the registration parameters  $\Theta$ . ECMPR is an advanced algorithm regarding the point registration problem. In [31], the authors demonstrated the advantage of this method in comparison with the most popular point registration approach, namely, Iterative Closest Point (ICP).

The crown of the mirrored tooth  $\{W'_n\}$  and the source tooth  $\{U'_m\}$  should be selected and serve as the model points and the observed points, respectively, which are the two sets of 3D points considered in ECMPR. This algorithm can match two shapes even though they are not exactly the same and their points are randomly distributed. Therefore, instead of taking time to segment the vertices on the crown, which is complex as the edge of the crown is a free curve, we simply sort the points in each set according to their  $z$ -coordinate and then select the upper  $1/N$  vertices for the teeth in the mandibular model and the lower  $1/N$  vertices for the teeth in the maxillary model. In our example, we select the upper  $1/N$  vertices of  $\{W'_n\}$  and  $\{U'_m\}$ , denoted by  $\{w'_i\}_{1 \leq i \leq M_2/N}$  and  $\{u'_j\}_{1 \leq j \leq N_2/N}$ . There are different number of points

in each set. An estimate of their 3D coordinates is available. The registration parameters  $\Theta$  can be evaluated by (11) with an ECM algorithm.

$$\Theta^{q+1} = \arg \min_{\Theta} \frac{1}{2} \sum_{j=1}^{M_2/N} \sum_{i=1}^{N_2/N} \alpha_{ji}^q \|u'_j - \mu_2(w'_j; \Theta^q)\|_{\Sigma}^2. \quad (11)$$

In (11),  $\alpha_{ji}$  is the posterior probabilities of assignment.  $\|w' - u'\|_{\Sigma}^2$  denotes the squared Mahalanobis distance, i.e.,  $(w' - u')^T \Sigma^{-1} (w' - u')$ , where  $\Sigma$  is a  $3 \times 3$  symmetric positive definite matrix.  $q$  denotes the  $q$ th iteration step. The 3D coordinates of the transformed model points in the  $q$ th iteration step are denoted by  $\mu_2(w'_i; \Theta^q)$  as follows:

$$\mu_2(w'_i; \Theta^q) = R^q w'_i + t^q, \quad (12)$$

Identity matrix and zero vector can be given to  $R$  and  $t$  for initialization. In E-step, the posterior  $\alpha_{ji}$  is evaluated with the current registration parameter  $\Theta^q$ . Each observed point can be assigned to a model point or to the outlier class with

$$Z_j = \arg \max_i \alpha_{ji}^q, \quad (13)$$

where  $Z_j = i$  indicates that  $u'_j$  matches  $w'_i$ , and  $Z_j = N_2/N + 1$  indicates that  $u'_j$  is an outlier. Then, in CM-step, the new registration parameter  $\Theta^{q+1}$  is updated. The iteration is stopped when the difference between  $\Theta^q$  and  $\Theta^{q+1}$  is small enough.

With the ECM algorithm, the mirrored tooth  $\{W'_n\}$  can be transformed to match the source tooth  $\{U'_m\}$ , as shown in Fig. 4(c), and the registration parameters  $\Theta$  according to the transformation  $\mu_2$  is obtained. The blue mesh and the red mesh do not coincide with each other fully because of two reasons. First, the braces that attach to each tooth have different shapes. Second, the spoke lines that segment the dental model can have different directions within a tolerance angle in interstice orientation, so that the left and right segmental edges of each mesh are different. These reasons can also explain why only the crowns are employed to estimate the transformation  $\mu_2$ .

### C. Fill the Partially Edentulous Space

With the properly estimated transformation  $\mu$ , the partially edentulous space can be filled with its symmetrical teeth.

In our example, the right lateral incisor is missing. As shown in Fig. 5(a), the partially edentulous position  $E$  is marked as the yellow mesh, which consists of the related tissues of the missing tooth, such as the gum, the brace, and the remnant of the missing tooth. The

symmetrical tooth  $\{V_k''\}$  of  $E$  is the left lateral incisor, which is marked as the pink mesh in Fig. 5(a).  $\{V_k''\}$  is segmented by its two spoke planes.

The mirror transformation matrix  $M$  in (10) is employed to flip  $\{V_k''\}$  as follows:

$$W_k'' = MV_k'' \quad (14)$$

$\{W_k''\}$  is the mirrored tooth and marked as the blue mesh in Fig. 5(b). It is transformed to the partially edentulous space  $E$  with the estimated transformation  $\mu_2$ , whose registration parameters  $\Theta$  are calculated by (11).

$$\hat{W}_k'' = RW_k'' + t \quad (15)$$

$\{\hat{W}_k''\}$  is called the implanted tooth, which is in the same location of  $E$ , but with different segmental edges. To have a smooth new model, first, the boundary of the implanted tooth  $\{\hat{W}_k''\}$  can be achieved by applying the same rigid transformation  $\mu$  parameterized by  $\{M, R, t\}$  to the two spoke planes of the symmetrical tooth  $\{V_k''\}$ . Then, a part of the dental model between the two transformed spoke planes can be segmented, which is denoted by  $E'$ .  $E'$  is at the same position of  $E$ , but with the same segmental edges as  $\{\hat{W}_k''\}$ . In this way, we create a space exactly fit  $\{\hat{W}_k''\}$ . Finally, we replace  $E'$  with the implanted teeth  $\{\hat{W}_k''\}$ . A complete dental model with symmetrical teeth  $\{V_k''\}$  implanted to the partially edentulous space  $E'$  is obtained.

Two narrow gaps exist between the implanted tooth and its neighbors because no facet joins the edge points. To obtain a continuous dental model, instead of creating the missed facets in the gap area, we generate a new triangulated mesh with all of the points of the complete new dental model, which is more convenient. In this project, the new meshes were generated with the Mimics software.

To summarize, the DRST algorithm is illustrated in Table I.

#### D. Alignment with Complete Dental Model

Dental occlusion reestablishment algorithm [19] can be employed to align the reconstructed complete dental model. Satisfactory alignment results are achieved.

### V. Results and Discussion

#### A. Synthetic Partially Edentulous Models

In this experiment, we employed two sets of digital dental models. Originally, they are dental sets with full dentition. We generated a sequence of the partially edentulous models

by extracting one to three different teeth from upper and lower dental model on each side. In detail, we extracted the lateral incisor, first premolar, and first molar to simulate the one missing tooth case. We extracted the lateral incisor and canine; canine and first premolar; and first premolar and second premolar to simulate the two missing teeth case. We extracted the lateral incisor, canine, and first premolar; canine, first premolar, and second premolar; and first premolar, second premolar, and first molar to simulate the three missing teeth case. We obtained 36 partially edentulous models from one full dentition model. It was applied to the two full dental models. Thus, in total, we had 72 partially edentulous models.

**1) Reconstruction Results**—The 72 partially edentulous models were reconstructed with our proposed DRST method.  $N$  in (11) is equal to 2 if the molars are employed for estimation; otherwise,  $N$  is set to 3. Fig. 6 demonstrates the results of dental reconstruction. In the first row, we give the original dental model with one, two, and three teeth missing. Their corresponding reconstructed dental models are shown in the second (front view) and third rows (top view). The implanted teeth fit the whole dental model decently, which is guaranteed by the accurate shape and size of the implanted teeth and the correct position of implantation. The continuous mesh models were generated by a business software (Mimics) and are given in the fourth row.

We quantitatively validate the reconstruction performance by measuring the Hausdorff Distance [36], which measures the distance between two sets of points [37], [38]. The Hausdorff Distance is employed to estimate the distance between the surface of implanted teeth  $\{\hat{W}_k''\}$  and the surface of the corresponding original teeth  $\{U_j''\}$  located in  $E_d$  and extracted synthetically. The average distance obtained from 10 randomly selected models is 0.73. When the size of one tooth is approximately  $8^3$ , the surface of implanted teeth is close to its ground truth.

**2) Occlusion Results**—To validate the occlusion, we first move the maxillary model of each model set to 112 different initial positions with 112 disarticulations, so that the maxilla and mandibula are no longer in MI. We then align them to the MI position with the full dentition occlusion algorithm and test the articulation. The 112 disarticulations are generated by combining 7 rotation matrices and 16 translation matrices. The rotation origin corresponds to the centroid of the mandibular teeth model. Seven rotation angles ( $-60^\circ$ ,  $-40^\circ$ ,  $-20^\circ$ ,  $0^\circ$ ,  $20^\circ$ ,  $40^\circ$ ,  $60^\circ$ ) are given. Each angle was applied with respect to the  $z$ -axis,  $y$ -axis, and  $x$ -axis orderly. The translation in the  $z$ -coordinate is  $40mm$  to be far enough vertically. The translations in the  $x$ -coordinate are  $-20mm$ ,  $-16mm$ ,  $-12mm$ , and  $-8mm$ . The translations in the  $y$ -coordinate are  $8mm$ ,  $12mm$ ,  $16mm$ , and  $20mm$ . With all these disarticulated models, the deformities in CMF can be represented adequately.

Three most commonly used landmarks [19] on maxillary model in clinical practices are chosen to test the alignment performance: the tooth crypt of the first right molar (A), the tooth crypt of the first left molar (B), and the central dental midline (C). When the model is at the original MI position, the coordinates of these landmarks are recorded and serve as the ground truth. We compared the coordinates of each landmarks after the models return from different initial positions. The mean translational deviations (deltas) and standard deviations

were calculated for different categories: one tooth missing and filled; two teeth missing and filled; three teeth missing and filled; all reconstructed models, which includes all of the models in the first three categories; and all partially edentulous models. They are listed in Table II. A translational deviation of less than  $0.5\text{mm}$  [17] is not clinically significant. However, most of the evaluated deltas of the partially edentulous dental model cannot reach this standard, and their maximum absolute mean error is  $3.2188\text{mm}$ . On the contrary, this requirement is satisfied by all of the occlusion results of the reconstructed dental model. Actually, most of the absolute errors are less than  $0.2\text{mm}$ . Their maximum absolute mean error is only  $0.3795\text{mm}$ . These data testify the excellent alignment performance of the reconstructed dental model. Thus, the proposed DRST approach can dramatically improve the occlusion results and achieve the correct surgical plan for the partially edentulous models.

## B. Real Partially Edentulous Model

We also test the approach with three real partially edentulous dental models. The occlusion results are shown in Fig. 7. The first patient lost the molars in her left mandibula [Fig. 7(a)]. The partially edentulous space was virtually filled with the molars in her right mandibula [Fig. 7(b)]. The second patient has a deformed second premolar in the left mandibula [Fig. 7(d)]. It was substituted with his second premolar in the right mandibula [Fig. 7(e)]. For these two patients, no teeth is missing in their maxilla, so we reconstruct only their mandibular model. The third patient lost his canine in the right maxilla [Fig. 7(g)] and the second molar in his right mandibula [Fig. 7(j)]. With the DRST method, the maxillary model is reconstructed with the canine in his left maxilla [Fig. 7(h)], and the mandibular model is reconstructed with the second molar in his left mandibula [Fig. 7(k)]. The continuous dental models are then obtained by generating a triangular mesh with the new point cloud. The reconstructed continuous models are shown in the last column in Fig. 7 according to each partially edentulous model. The real partially edentulous models are not as symmetrical as the synthetic partially edentulous models because the patients cannot use the both sides of their teeth equally when some teeth are missing. However, reasonable reconstruction has been achieved in each case. The implanted teeth have suitable shapes and sizes and are implanted into the correct position even though the transformed braces and gums may not fit the curvature in the other side because the shape of braces and gums may not be symmetrical. Nonetheless, this fit is not important because only the teeth will be considered in the alignment algorithm.

The mandibular model of each patient has been disarticulated to 112 initial positions as stated in Section V-A. When they are aligned, the errors of each landmark are computed. The same alignment experiments are carried on with the dental model sets before the reconstruction. The errors are collected as well. For comparison, the two sets of errors obtained with the reconstructed models and the partially edentulous models are listed in Table III. Eight of nine errors obtained with the partially edentulous models are larger than  $0.5\text{mm}$  [17], which means that the occlusion with the partially edentulous models cannot provide correct results. However, with the reconstructed models, the alignment errors of each landmark in each direction are less than  $0.5\text{mm}$  [17] and satisfy the standard.

Therefore, the DRST method can accurately obtain a complete dental model, thereby leading to correct alignment.

## VI. Discussion and Conclusion

Our approach is different from the other teeth reconstruction approaches.

First, the proposed solution is novel. In the previous methods [24], [25], a template model of the concerned tooth is required, which is trained from a set of tooth samples. In this step, the landmarks on each sample tooth should be marked manually. Then, a tooth is reconstructed with its neighbors and the template model. For example, in [25], the method is developed to reconstruct the missing part of a broken tooth crown, and to reconstruct the crown of a whole missing tooth or several teeth. This method has to build a model of the shape variability of the teeth, their neighbors, and their antagonists. In their experiment, 12 samples are applied to train a model for one tooth. Landmarks are manually assigned to each sample. Then, Bayes method is employed to propose the reconstruction of missing teeth. Based on the known data of the remaining tooth crown or the neighboring teeth, the most probable shape of the missing teeth is inferred by matching to the established shape model. In this method, to reconstruct one tooth, the landmarks in 12 samples should be marked manually, which is time-consuming. Most importantly, each template model is obtained from 12 samples, which cannot provide enough information to describe the diversified properties of the tooth of different patients. The shape of a tooth varies at different age. The uniformed tooth model based on the limited 12 samples is not qualified to serve as the template for all patients because it can not fit the existing individual anatomy of each patient even after optimization of the concerned dental model.

Second, the addressed problem is not the same. Most of the previous methods [23], [24] are developed to restore the tooth crown decayed by cavities. They can reconstruct only teeth with remnants. If a tooth is missing totally, then it cannot be reconstructed. In [25], the approach is enhanced to reconstruct the whole missing tooth. In our proposed method, the partially edentulous position can be reconstructed even when the whole tooth is missing.

Lastly, the ultimate goal of our approach is different. The previous methods [23]–[25] aim to reconstruct the tooth for chewing purpose. The artificial tooth or restored tooth crown calculated by the methods should be realized in real operation. However, our goal is to reestablish dental occlusion. In real surgery, there is no need to reconstruct the missing teeth physically. The partially edentulous mandibula or maxillia will be aligned to the MI position without being filled according to the occlusion plan.

Our approach is different from the other dental occlusion approaches as well. The previous occlusion approaches [16]–[19] can only align the mandibula and maxilla with full dentition. With the proposed DRST method, our occlusion approach can align the partially edentulous dental model to MI position successfully. With respect to the mean error of approximately  $0.1\text{ mm}$  in the most recent work [19] obtained with full dentition, our errors reported in Tables II and III are comparable.

The limitation of our approach is that the symmetrical teeth of the partially edentulous space has to exist. Moreover, the teeth pair for the estimation of transformation has to exist. Nevertheless, these requirements are usually satisfied. Most of the partially edentulous dental models are qualified to be treated with the proposed DRST approach. For the serious asymmetric situation, we would propose to fill the partially edentulous space with the simulated teeth which are generated from statistic teeth models, then the dental occlusion reestablishment algorithm [19] can be applied to achieve alignment results.

In this paper, we introduced the innovative DRST approach, which can properly reconstruct the partially edentulous model by virtually implanting the symmetrical counterpart to the partially edentulous space. The symmetrical counterpart provides an ideal substitute of the original missing teeth. The transformation is estimated with another pair of symmetrical teeth. Digital dental occlusion can be reestablished with the virtually reconstructed models. Satisfactory reconstruction and occlusion results have been demonstrated with both synthetic and real partially edentulous dental models.

## Acknowledgments

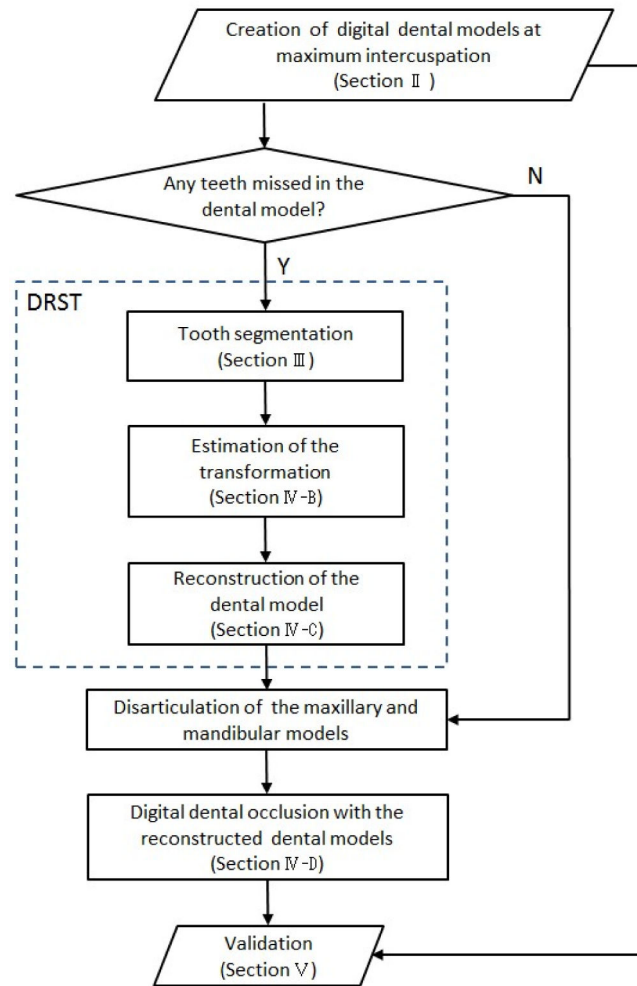
This work was supported by NIH (National Institutes of Health) R01 grant DE022676.

## References

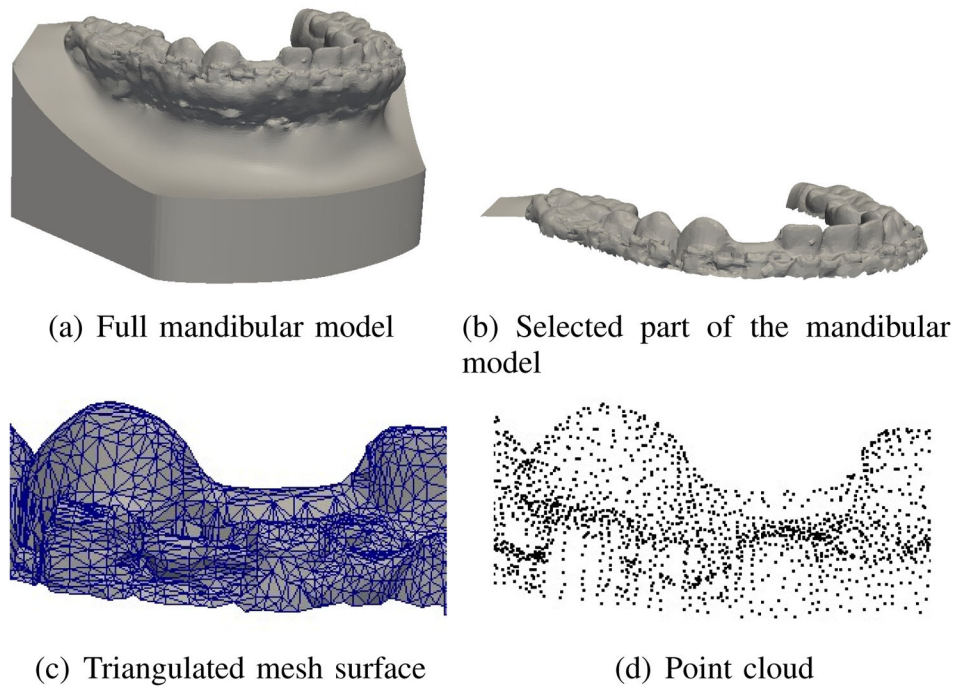
1. Zachow S, Hege HC, Deuffhard P. Computer assisted planning in cranio-maxillofacial surgery. *CIT Journal of computing and information technology*. 2006; 14(1):53–64.
2. Bill J, Reuther J. Rapid prototyping in planning reconstructive surgery of the head and neck. review and evaluation of indications in clinical use. *Mund-, Kiefer-und Gesichtschirurgie: MKG*. 2004; 8(3):135–153.
3. Xia JJ, Phillips CV, Gateno J, Teichgraeber JF, Christensen AM, Gliddon MJ, Lemoine JJ, Liebschner MA. Cost-effectiveness analysis for computer-aided surgical simulation in complex cranio-maxillofacial surgery. *Journal of oral and maxillofacial surgery*. 2006; 64(12):1780–1784. [PubMed: 17113445]
4. Gassner R, Tuli T, Hächl O, Rudisch A, Ulmer H. Cranio-maxillofacial trauma: a 10 year review of 9543 cases with 21067 injuries. *Journal of Cranio-Maxillofacial Surgery*. 2003; 31(1):51–61. [PubMed: 12553928]
5. Mithani SK, Hilaire HS, Brooke BS, Smith IM, Bluebond-Langner R, Rodriguez ED. Predictable patterns of intracranial and cervical spine injury in craniomaxillofacial trauma: analysis of 4786 patients. *Plastic and reconstructive surgery*. 2009; 123(4):1293–1301. [PubMed: 19337097]
6. Al-Khateeb T, Abdullah FM. Craniomaxillofacial injuries in the united arab emirates: a retrospective study. *Journal of oral and maxillofacial surgery*. 2007; 65(6):1094–1101. [PubMed: 17517291]
7. Kawamoto HK Jr. Surgical correction of dentofacial deformities. *Plastic and Reconstructive Surgery*. 1988; 82(4):714.
8. Wade AL, Dye JL, Mohrle CR, Galarnau MR. Head, face, and neck injuries during operation iraqi freedom ii: results from the us navy-marine corps combat trauma registry. *Journal of Trauma-Injury, Infection, and Critical Care*. 2007; 63(4):836–840.
9. Petroff MA, Burgess L, Anonsen CK, Lau P, Goode RL. Cranial bone grafts for post-traumatic facial defects. *The Laryngoscope*. 1987; 97(11):1249–1253. [PubMed: 3312882]
10. Okeson, JP. Management of temporomandibular disorders and occlusion. Elsevier Health Sciences; 2007.
11. Proffit W, Fields H Jr, Moray L. Prevalence of malocclusion and orthodontic treatment need in the united states: estimates from the nhanes iii survey. *The International journal of adult orthodontics and orthognathic surgery*. 1997; 13(2):97–106.

12. Gateno J, Xia JJ, Teichgraber JF, Christensen AM, Lemoine JJ, Liebschner MA, Gliddon MJ, Briggs ME. Clinical feasibility of computer-aided surgical simulation (cass) in the treatment of complex cranio-maxillofacial deformities. *Journal of Oral and Maxillofacial Surgery*. 2007; 65(4): 728–734. [PubMed: 17368370]
13. Motohashi N, Kuroda T. A 3d computer-aided design system applied to diagnosis and treatment planning in orthodontics and orthognathic surgery. *The European Journal of Orthodontics*. 1999; 21(3):263–274. [PubMed: 10407535]
14. Xia J, Ip HH, Samman N, Wang D, Kot CS, Yeung RW, Tideman H. Computer-assisted three-dimensional surgical planning and simulation: 3d virtual osteotomy. *International journal of oral and maxillofacial surgery*. 2000; 29(1):11–17. [PubMed: 10691136]
15. Altobelli DE, Kikinis R, Mulliken JB, Cline H, Lorensen W, Jolesz F, et al. Computer-assisted three-dimensional planning in craniofacial surgery. *Plastic and Reconstructive Surgery*. 1993; 92(4):576–585. [PubMed: 8356120]
16. Zhang, C., Chen, L., Zhang, F., Zhang, H., Feng, H., Dai, G. *Digital Human Modeling*. Springer; 2007. A new virtual dynamic dentomaxillofacial system for analyzing mandibular movement, occlusal contact, and tmj condition; p. 747-756.
17. Hiew, LT., Ong, SH., Foong, KWC. Optimal occlusion of teeth. *Control, Automation, Robotics and Vision*, 2006. ICARCV'06. 9th International Conference on; IEEE; 2006. p. 1-5.
18. DeLong R, Ko CC, Anderson GC, Hodges JS, Douglas W. Comparing maximum intercuspal contacts of virtual dental patients and mounted dental casts. *The Journal of prosthetic dentistry*. 2002; 88(6):622–630. [PubMed: 12488856]
19. Chang YB, Xia JJ, Gateno J, Xiong Z, Zhou X, Wong ST. An automatic and robust algorithm of reestablishment of digital dental occlusion. *Medical Imaging, IEEE Transactions on*. 2010; 29(9): 1652–1663.
20. Douglass CW, Shih A, Ostry L. Will there be a need for complete dentures in the united states in 2020? *The Journal of prosthetic dentistry*. 2002; 87(1):5–8. [PubMed: 11807476]
21. Emami E, de Souza RF, Kabawat M, Feine JS. The impact of edentulism on oral and general health. *International journal of dentistry*. 2013; 2013
22. Cooper LF. The current and future treatment of edentulism. *Journal of Prosthodontics*. 2009; 18(2): 116–122. [PubMed: 19254301]
23. Gurke S. Restoration of teeth by geometrically deformable models. 1997
24. Blanz, V., Mehl, A., Vetter, T., Seidel, H-P. A statistical method for robust 3d surface reconstruction from sparse data. *3D Data Processing, Visualization and Transmission*, 2004. 3DPVT 2004. Proceedings. 2nd International Symposium on; IEEE; 2004. p. 293-300.
25. Sporrying J, Jensen KH. Bayes reconstruction of missing teeth. *Journal of Mathematical Imaging and Vision*. 2008; 31(2–3):245–254.
26. Bailit H. Dental variation among populations. an anthropologic view. *Dental Clinics of North America*. 1975; 19(1):125–139. [PubMed: 1053731]
27. So LL. Unusual supernumerary teeth. *The Angle Orthodontist*. 1990; 60(4):289–292. [PubMed: 2256567]
28. Sonick M. Esthetic crown lengthening for maxillary anterior teeth. *Compendium*. 1997; 18(8):807–812. [PubMed: 9533339]
29. Kondo T, Ong S, Foong KW. Tooth segmentation of dental study models using range images. *Medical Imaging, IEEE Transactions on*. 2004; 23(3):350–362.
30. Paulus D, Wolf M, Meller S, Niemann H. Three-dimensional computer vision for tooth restoration. *Medical image analysis*. 1999; 3(1):1–19. [PubMed: 10709694]
31. Horaud R, Forbes F, Yguel M, Dewaele G, Zhang J. Rigid and articulated point registration with expectation conditional maximization. *Pattern Analysis and Machine Intelligence, IEEE Transactions on*. 2011; 33(3):587–602.
32. Besl, PJ., McKay, ND. Robotics-DL tentative. *International Society for Optics and Photonics*; 1992. Method for registration of 3-d shapes; p. 586-606.
33. Sharp GC, Lee SW, Wehe DK. Maximum-likelihood registration of range images with missing data. *Pattern Analysis and Machine Intelligence, IEEE Transactions on*. 2008; 30(1):120–130.

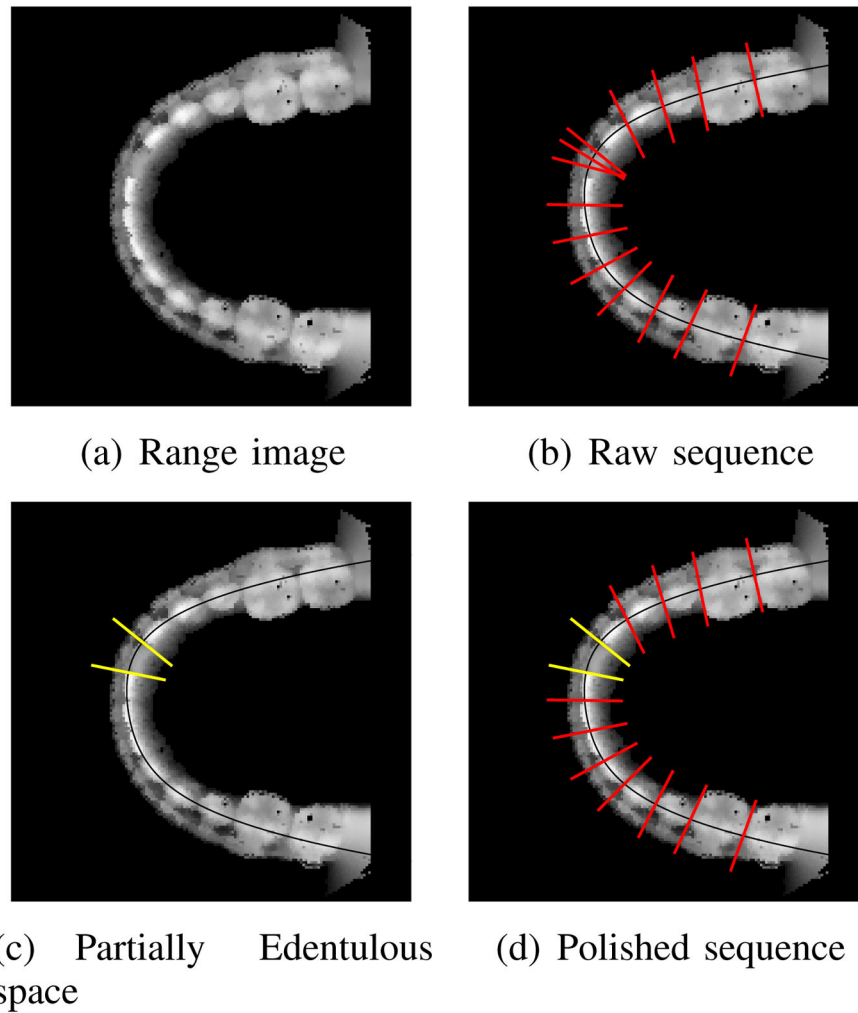
34. Rangarajan, A., Chui, H., Bookstein, FL. Information Processing in Medical Imaging. Springer; 1997. The softassign procrustes matching algorithm; p. 29-42.
35. Chui, H., Rangarajan, A. A feature registration framework using mixture models. Mathematical Methods in Biomedical Image Analysis, 2000. Proceedings. IEEE Workshop on; IEEE; 2000. p. 190-197.
36. Aspert N, Santa Cruz D, Ebrahimi T. Mesh: measuring errors between surfaces using the hausdorff distance. ICME. 2002; (1):705–708.
37. Hung WL, Yang MS. Similarity measures of intuitionistic fuzzy sets based on hausdorff distance. Pattern Recognition Letters. 2004; 25(14):1603–1611.
38. Schütze O, Esquivel X, Lara A, Coello CAC. Using the averaged hausdorff distance as a performance measure in evolutionary multiobjective optimization. Evolutionary Computation, IEEE Transactions on. 2012; 16(4):504–522.



**Fig. 1.** Overview of the procedure for the reconstruction-based digital dental occlusion of the partially edentulous dentition.



**Fig. 2.** Digital dental model. (a) Full mandibular model scanned by the 3D laser surface scanner, whose right lateral incisor was missed synthetically. (b) Interested part of the full model, which is employed in the proposed approach. (c) Triangulated mesh surface around the missing tooth. (d) Point cloud on the model surface, which is formed by the vertices of the triangulated mesh.

**Fig. 3.**

Dental segmentation. (a) Range image of the digital dental model in Fig. 2(b). (b) Sequence of raw spokes (red). Some of the spokes are located in the partially edentulous position by mistake; the others indicate each tooth correctly. The black curve is the dental arch curve. (c) The two articulated spokes (yellow) indicate the partially edentulous position. (d) Sequence of the polished spokes (both red and yellow), which correctly segment each tooth and the partially edentulous position.

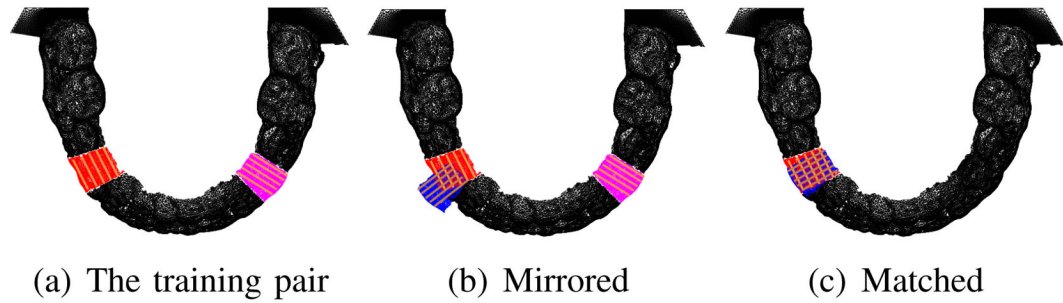


**Fig. 4.**

Estimate the transformation with a pair of teeth. Consider the partially edentulous dental model in Fig. 2(b), where the right lateral incisor was missed. (a) The right first premolar and the left first premolar were selected as the source tooth (red) and the symmetrical tooth (pink) for estimation. The two teeth are symmetrical with each other and existed on both sides. (b) The symmetrical tooth (pink) was flipped to the other side as the mirrored tooth (blue) by a mirror transformation about the  $y$ - $O$ - $z$  plane. (c) The mirrored tooth (blue) was transformed to match the source tooth (red). The parameters that define the transformation were estimated in this way. The concerned areas are highlighted with stripes.

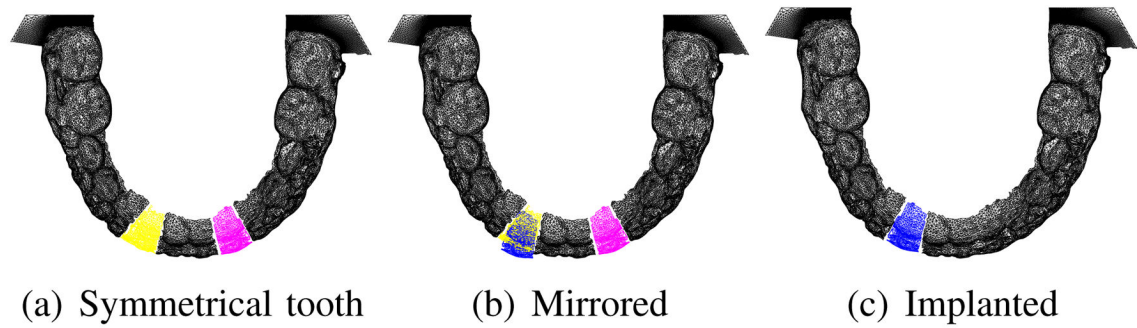


**Fig. 5.**

Fill the partially edentulous space with its symmetrical tooth. Consider the partially edentulous dental model in Fig. 2(b), where the right lateral incisor was missed. (a) The left lateral incisor was selected as the symmetrical tooth (pink) of the partially edentulous position (yellow), where is the related tissue of the missing tooth. (b) The symmetrical tooth (pink) was flipped to the other side as the mirrored tooth (blue) by a mirror transformation about the  $y-O-z$  plane. (c) The mirrored tooth (blue) was virtually implanted to the partially edentulous position with the transformation estimated in Fig. 4. The related tissue of the missing tooth was deleted.

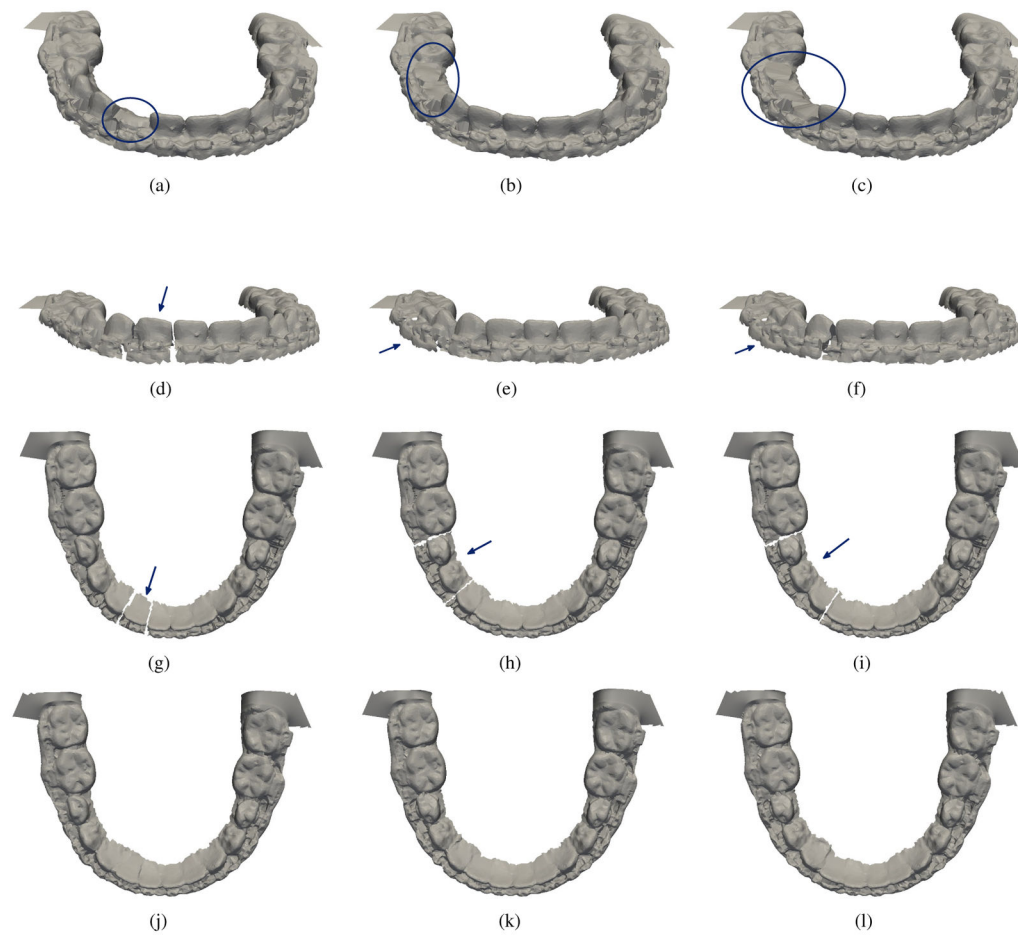


**Fig. 6.**

Reconstruction of three synthetic partially edentulous examples. The first row gives three dental models with 1, 2, and 3 teeth extracted. They are produced from the same dental model, which is with full dentition. Specifically, in (a), the right lateral incisor is virtually extracted; in (b), the right first premolar and the right second premolar are virtually extracted; in (c), the right canine, the right first premolar, and the right second premolar are virtually extracted. The partially edentulous space is marked by ellipse. Their corresponding reconstructed dental models are shown in the second (top view) and third rows (front view). The reconstructed entity is pointed out by arrow. The corresponding continuous dental models are in the fourth row.

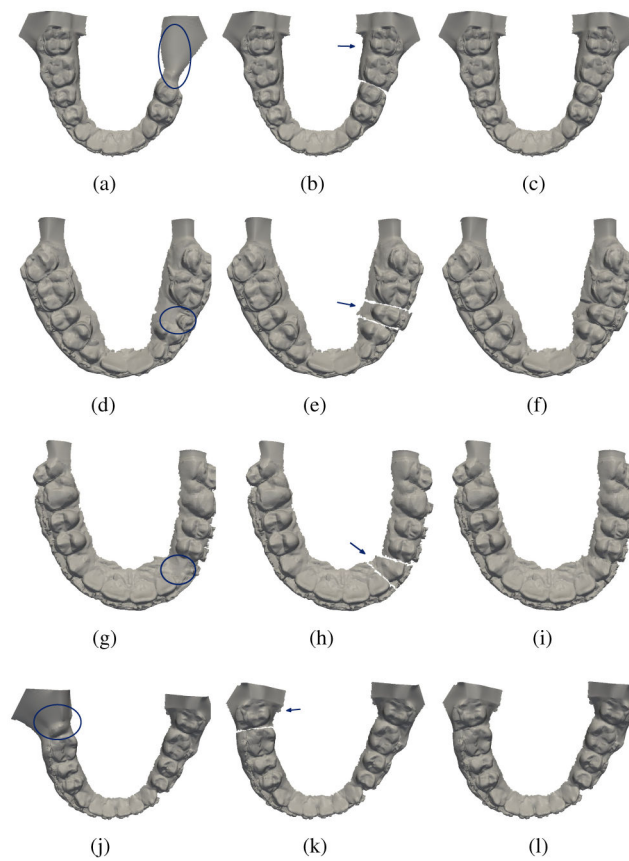


**Fig. 7.**

Reconstruction of four real partially edentulous models. The first column shows the original partially edentulous models. The partially edentulous space is marked by ellipse. Their corresponding reconstructed dental models are shown in the second column. The reconstructed part is pointed out by arrow. The corresponding continuous models are in the third column. The four real dental models are from three patients. The first patient lost the molars in her left mandibula (the first row). No teeth is missing in her maxilla. The second patient has a seriously deformed second premolar in his left mandibula (the second row). No teeth is missing in his maxilla. The third patient lost the canine in his right maxilla (the third row) and the second molar in his right mandibula (the fourth row).

TABLE I

## Algorithm of Dental Reconstruction with Symmetrical Teeth.

---

**Input:** A partially edentulous dental model (mandibula or maxilla)

**Output:** A reconstructed dental model with full dentition

1. *Tooth segmentation.*

Segment each tooth and the partially edentulous positions  $E_a$  ( $a = 1, \dots, K$  where  $K$  is the total number of the partially edentulous positions).

**For each**  $E_a$

2. *Estimation.*

- a. Select and segment a pair of symmetrical teeth  $\{U'_m\}$  and  $\{V'_n\}$ .  $\{U'_m\}$  is on the same side of  $E_a$ ;  $\{V'_n\}$  is on the other side.
- b. Implement mirror transformation  $\mu_1$  with  $M$  in (10).  $W'_n = MV'_n$ .
- c. Estimate the transformation  $\mu_2$  by (11), which makes  $\hat{W}'_n = RW'_n + t$ , and  $\{\hat{W}'_n\}$  matches  $\{U'_m\}$ .

3. *Reconstruction.*

- a. Segment the teeth  $\{V''_k\}$ , which is in the symmetrical position of  $E_a$ .
- b. Implement mirror transformation  $\mu_1$  with  $M$  in (10).  $W''_k = MV''_k$ .
- c. Implant to  $E_a$  with the estimated  $\Theta$ .  $\hat{W}''_k = RW''_k + t$ .

**Loop**

4. *Generate the continuous mesh.*

Remark:  $\{V\}$  is not a previously calculated  $\{\hat{W}''\}$  for the specific case where a tooth is missing on both sides of the arc and their neighbouring tooth is the symmetrical tooth of the other missing one.

---

Translational deviations in the simulation of alignment with the synthetic partially edentulous models and the corresponding reconstructed models.

**TABLE II**

Marker axis	One tooth		Two teeth		Three teeth		Reconstructed		Partially Edentulous		
	Mean (mm)	SD	Mean (mm)	SD	Mean (mm)	SD	Mean (mm)	SD	Mean (mm)	SD	
(A',A)	x	-0.0336	0.1921	-0.1244	0.2101	-0.2721	0.2683	-0.1263	0.2389	1.5028	0.8568
	y	-0.0384	0.1927	-0.1273	0.2090	-0.2682	0.2634	-0.1282	0.2360	1.1988	0.7316
	z	-0.3614	0.1410	-0.3069	0.0110	-0.4676	0.2069	-0.3689	0.1500	-3.2188	1.4332
(B',B)	x	-0.2434	0.1573	-0.1960	0.1704	-0.1013	0.2350	-0.1906	0.1925	0.6769	0.9568
	y	0.1837	0.2466	0.1529	0.0884	0.2955	0.1685	0.2011	0.1922	0.4470	1.4536
	z	-0.2443	0.1203	-0.0159	0.0741	0.1001	0.1560	0.0111	0.1283	0.6375	0.4062
(C',C)	x	0.0941	0.1693	0.0668	0.1704	0.0236	0.1596	0.0666	0.1695	-0.2440	0.2381
	y	-0.2443	0.2394	-0.1395	0.0509	-0.0676	0.1623	-0.1623	0.1873	-0.9279	0.6565
	z	0.0634	0.1165	0.1069	0.0842	0.0726	0.1977	0.0812	0.1345	-0.7744	0.5197

Translational deviations in the simulation of alignment with the real partially edentulous models and the corresponding reconstructed dental models.

**TABLE III**

Marker	axis	Reconstructed		Partially Edentulous	
		Mean (mm)	SD	Mean (mm)	SD
(A',A)	x	-0.0278	0.0030	0.6547	0.0030
	y	-0.0542	0.0030	0.5219	0.0040
	z	-0.3007	0.0027	-0.7208	0.0078
(B',B)	x	-0.0751	0.0025	-1.2436	0.0032
	y	0.4004	0.0033	0.8951	0.0092
	z	0.0980	0.0027	-0.2541	0.0028
(C',C)	x	-0.1603	0.0028	-0.1569	0.0040
	y	-0.3676	0.0027	-0.5413	0.0153
	z	0.3065	0.0032	0.1354	0.0076